

# Photodegradation, Antibacterial & Antioxidant Assessment of Multifunctional Zinc Oxide Metal Nanoparticles Using *Smilax aspera* Leaf Extract: An Eco Approach

Negi A<sup>1</sup>, Rana P<sup>1</sup>, Gangwar R<sup>2</sup>, Vishwakarma RK<sup>1</sup>, Negi DS<sup>\*1</sup> and Khoobchandani M<sup>3</sup>

<sup>1</sup>Department of Chemistry, H.N.B. Garhwal University, India

<sup>2</sup>Department of Microbiology, H.N.B. Garhwal University, Srinagar (Garhwal), Uttarakhand, India

<sup>3</sup>Institute of Green Nanotechnology, University of Missouri, Columbia, MO, 65212, USA

\*Corresponding author: Negi DS, Department of Chemistry, H.N.B. Garhwal University (A Central University), India, Tel: +919719738317, E-mail: devendra\_negi@yahoo.com

**Citation:** Negi A, Rana P, Gangwar R, Vishwakarma RK, Negi DS, et al. (2020) Photodegradation, Antibacterial & Antioxidant Assessment of Multifunctional Zinc Oxide Metal Nanoparticles Using *Smilax aspera* Leaf Extract: An Eco Approach. J Pharma Drug Develop 7(2): 202

**Received Date:** November 02, 2020 **Accepted Date:** December 21, 2020 **Published Date:** December 23, 2020

## Abstract

The endeavor of this research accounts for a superficial green route scheme by using an extract of leaves of *Smilax aspera* as a stabilizing and capping agent. Zinc Oxide nanoparticles (ZnO-NPs) were examined through UV-visible Spectrophotometer, X-Ray Diffraction (XRD), EDX (Energy Dispersive X-rays spectroscopy), Scanning Electron Microscopy (SEM), Transmission Electron Microscopy (TEM). The NPs demonstrate potential photo catalytic activity for the degradation of Methyl Orange (MO) and Methylene Blue (MB) dyes upon exposure to sunlight. We investigated the antibacterial action of ZnO-NPs against two gram positive and *Staphylococcus aureus*, *Streptococcus pneumoniae* and three-gram negative microbes viz, *Klebsiella pneumoniae*, *Escherichia coli* and *Pseudomonas aeruginosa* correspondingly). In general, the trial result proposes that ZnO-NPs could be created as an antibacterial specialist against a wide scope of microorganism to oversee and stay away from scattering and determination of bacterial contaminations. On the other hand, 2,2-diphenyl-1-picrylhydrazyl (DPPH) radical scavenging evaluation of obtained nanoparticles resulted percentage inhibition in concentration dependent mode.

**Keywords:** ZnO NP; UV; Tauc-plot; XRD; SEM; EDX; TEM; Photodegradation; Antibacterial; Antioxidant Efficacy

## Introduction

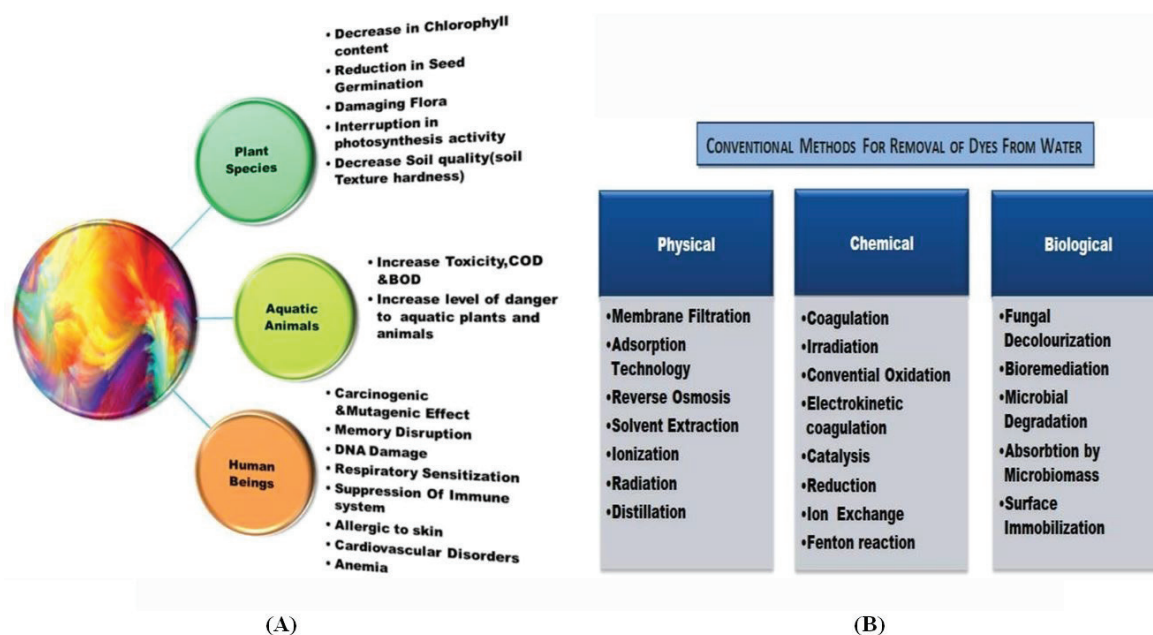


Figure 1: (A): Hazards of Dye; (B): Methods for removing dyes

During the dyeing process, the color extras agitated to the textures clear out with water while flushing. These unstable dyes contain organic and inorganic chemicals in elevated concentrations, some of which are non-biodegradable and dangerous to the atmosphere. The poisonous nature of dyes causes death to the soil microorganisms and influences the agrarian yield [1,2]. Diminution in light dispersion through water decreases photosynthetic activity due to oxygen deficiency which in turn de-regulates aquatic biota. Dyes have unending effects upon organisms, depending on the exposure time and concentration they can cause skin irritation, vomiting, gastritis, permanent blindness, hypertension and respiratory distress (Figure 1a) [3-5]. Different physical, synthetic, and natural methods for staining of color effluents have been developed over the last years (Figure 1b). Destructive techniques such as chemical oxidation and advanced oxidation processes (AOPs) may overcome these issues but these are costly and degradation is found to be deficient. Photocatalysis under visible-light irradiation is one of the most competent and inexpensive methods as it does not require additional synthetic substances and the fundamental part is visible light [6-8].

In this mechanism the dye excitation due to solar exposure from the ground state (Dye) to the triplet excited state (Dye\*) takes place. In its initial step, photo-generated holes and electrons are formed in the valence band ( $h^+VB$ ) and the conduction band ( $e^-CB$ ) individually. Subsequently, these photogenerated charge transporters at that point reacts with water or dissolved oxygen to produce reactive oxidizing species such as OH radicals and  $O_2^-$  that break down dyes into smaller molecules [9-11] (Figure 2).

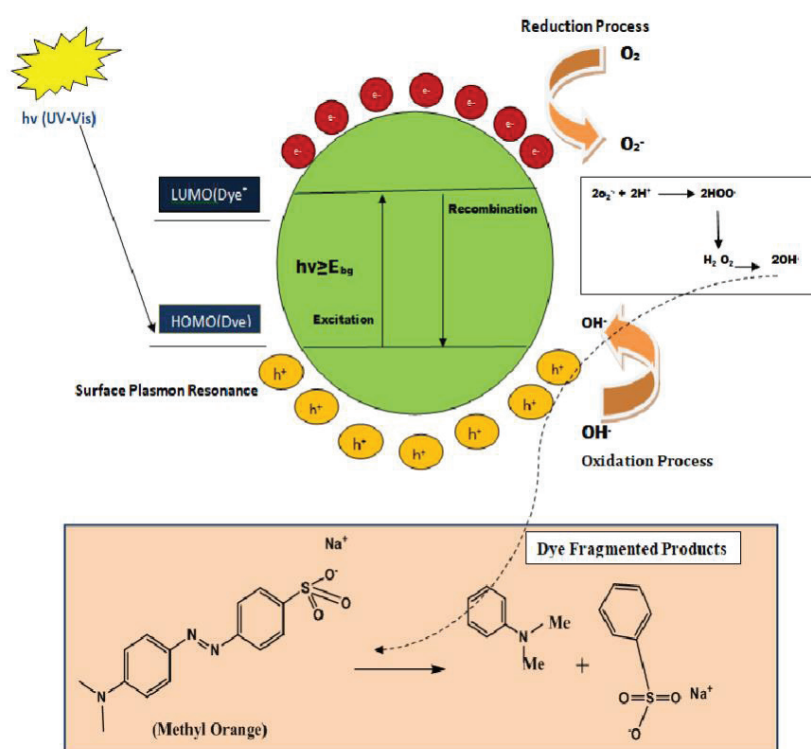


Figure 2: Scheme of photodegradation

Another serious issue alongside natural consumption is the losses because of post-careful injury contaminations dependent on microbial microorganisms. Studies have revealed that the event of post careful injury contaminations goes from 14.8% to 60% which are brought about by *S. aureus* and *P. aeruginosa* (the most well-known microbes). Irrespective of this, Antibiotic contradiction has become a significant issue as uncovered by various health organizations [12-15].

With the developing section of time, a critical need was felt for the advancement of inventive techniques to beat these issues. The ongoing period of material science and innovation have seen the development of another logical space viz. nanotechnology. A flexible solution for the mentioned issues has been given by metallic nanoparticles (MNPs). Surface plasmon resonance (SPR), minuscule size, surface charge, enormous surface territory to the volume proportion, large bandgap and characteristic dependability are a portion of the traits attributable to which these NPs have excellent antibacterial and photocatalytic properties [16,17]. For the formation of MNPs, Green Synthesis measures have gotten a lot of consideration as a suitable option as it has a few preferences over customary techniques as the green strategy is practical, eco-accommodating, one pot synthesis and required normal conditions [18,19].

Green Method is a type of bottom up approach where natural material is used as a fundamental material. The organic concentrates contain auxiliary phytoconstituents and biomolecules, which helps in controlling the stabilization and kinetic growth of NPs by acting as a capping and reducing agent [20,21].

*Smilax aspera* (*S. aspera*) notable as sarsaparilla is an evergreen shrub of Smilacaceae family, consists a few phytoconstituents. Flavonoids and tannins have been reported in rhizome and foliage of *Smilax aspera*. Anthocyanins in the berries and Steroidal Saponins subsp. mauritanica (POIR.) ARCANG. (Liliaceae), along with the known curillin G, asparoside E, asparoside A, asparoside B from the roots were removed and distinguished. These optional metabolites show antioxidant, antifungal, antiproliferative properties [22-25].

## Methodology

### Material

Leaves of *Smilax aspera* were gathered from Pauri Garhwal, Uttarakhand (Figure 3). Zinc Acetate ( $Zn(CH_3COO)_2 \cdot 6H_2O$ ), DPPH (2,2-Diphenyl-1-picrylhydrazyl), Butylated hydroxytoluene (BHT) was secured from Sigma Aldrich and NaOH, Methylene Blue ( $C_{16}H_{18}ClN_3S$ ), Methylene Orange ( $C_{14}H_{14}N_3NaO_3S$ ) were acquired from Fischer Scientific. Double Distilled water was utilized all through the investigation.

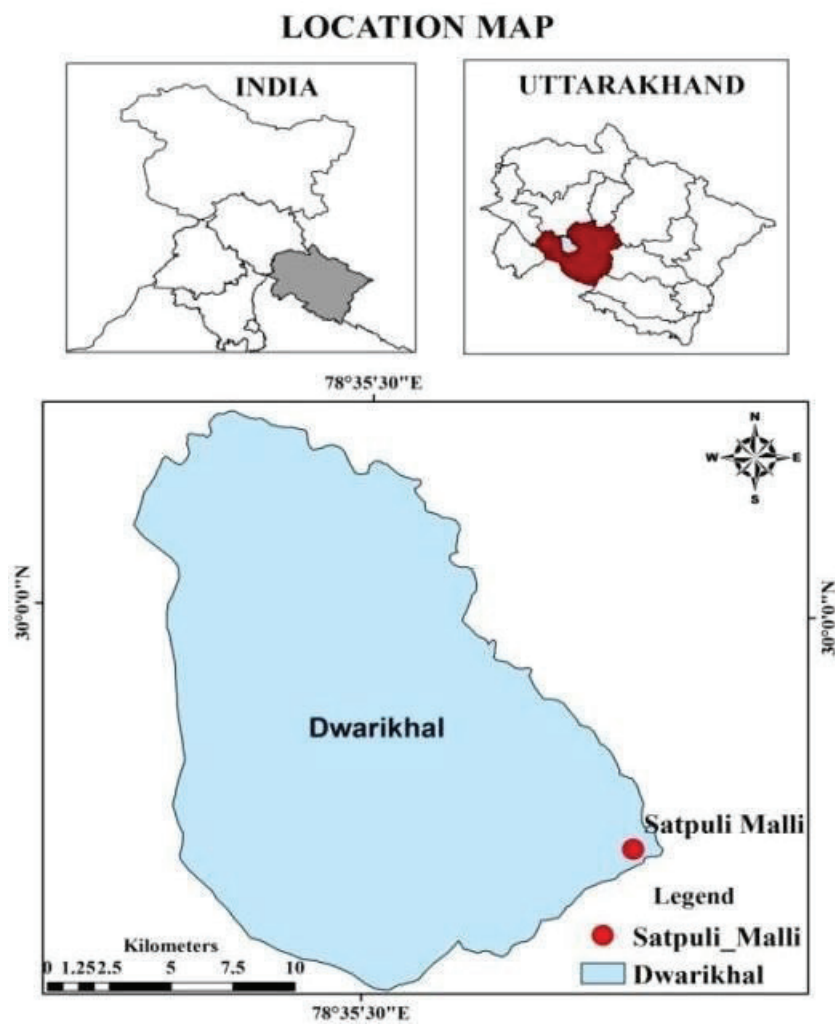


Figure 3: Field location map

### Plant Extraction Preparation

Freshly collected leaves were washed thoroughly with water to remove adhesive impurities and then air-dried to eliminate the left-over moisture. The leaves were powdered in a mechanical grinder and sieved powder was used for all studies. Various concentrations (3,5,7 and 10% w/v) of leaves extract solution were prepared by mixing in 250mL of distilled water in a 500 mL Erlenmeyer flask and heated the solution to 80 °C for 40 minutes. The extract was cooled down and centrifuged at 4000rpm to remove unwanted residue and adjusted to 100mL by adding distilled water and filtered using Whatman no.1 filter paper. The concentrate was put away at 40 °C to be utilized for additional trials.

### Green Synthesis of Zinc Oxide Nanoparticles

25 ml of the plant extract was heated at 60 °C for 15 min under magnetic stirring and then 50 ml solution of about 0.1 M Zn ( $(CH_3COO)_2 \cdot 6H_2O$ ) in double distilled water was added dropwise to the plant extract. The mixture was heated under continuous

stirring for 20 min and few drops of NaOH added for maintaining the pH of the solution. After the complete dissolution of the mixture  $Zn(OH)_2$  precipitation settled to the bottom and the supernatant was discarded. The light-yellow solid obtained was separated from the solution by centrifuging at 3500 rpm for 10 min and cleansed with distilled water repeatedly to remove the impurities. Obtained material thus subjected to calcination at 200 °C for 4 hr was further mashed in a mortar-pestle to get a finer nature for characterization (Figure 4).

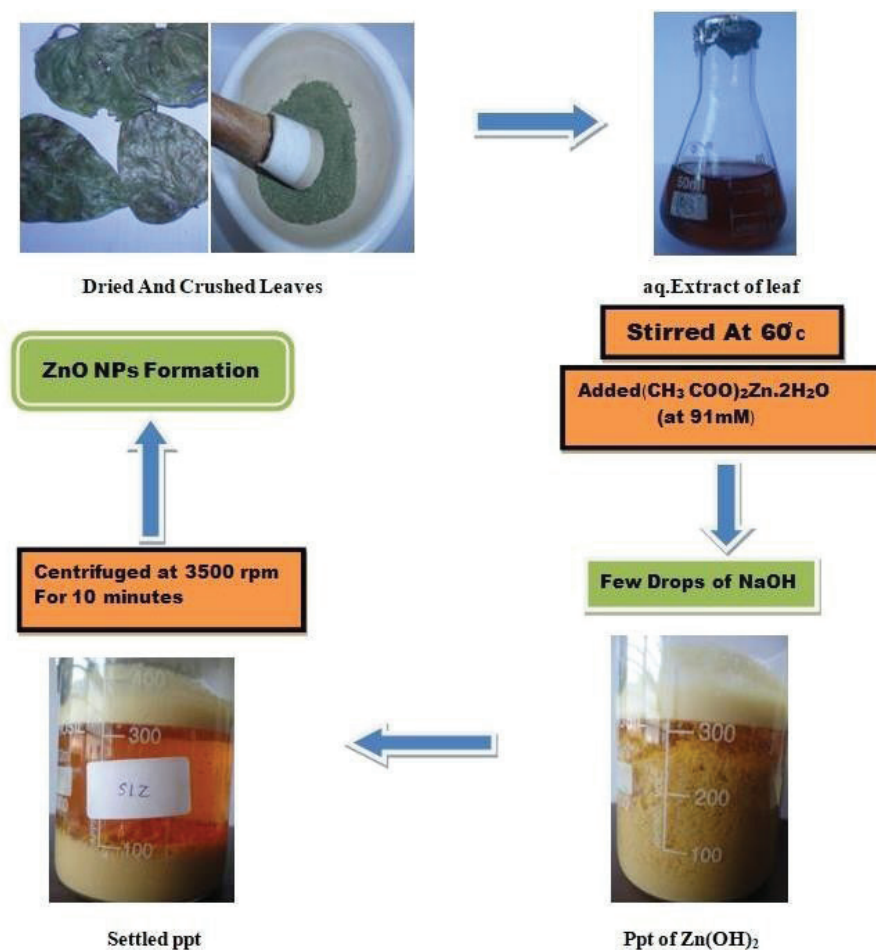


Figure 4: Pictorial representation of the process used

## Characterization Techniques

**Ultraviolet-Visible Spectroscopy (UV-Vis):** The biosynthesis of ZnO-NPs was recorded by measuring UV-Vis spectra of the aqueous solutions (1:3 diluted) obtained via reaction mixture. Characterization was done with an Elico SL UV-visible spectroscope within a wavelength range of 200–800 nm at fine resolution. Blank reading using Distilled water was taken.

**X-Ray Powder Diffraction Spectroscopy (XRD):** The XRD analysis of purified powdered was subjected to an X-ray diffractometer (PANalytical, X\*PERT PRO), using radiation of  $CuK\alpha$  with 1.54 Å wavelength. XRD was used to analyze the crystalline nature of nanoparticles and for providing information us on unit cell dimensions. XRD also determined the crystalline size of nanoparticles using Debye Scherrer's equation:

$$D = K\lambda / \beta \cos\theta$$

Where D= Crystallite size, K= shape factor,  $\lambda$  = wavelength,  $\beta$  = full width at half maxima and  $\theta$  = angle.

**Scanning Electron Microscopy (SEM) Analysis:** The Surface morphology of the product was studied by employing (CARI ZEISS, MA15/EVO18) Scanning Electron Microscope.

**Energy Dispersive X-ray (EDX) Pattern:** The chemical composition of the nanoparticles was determined by EDX pattern followed by SEM analysis.

**Transmission Electron Microscopy (TEM) Analysis:** The grain size of the prepared NPs was determined using FEI Tecnai TF20 equipped with FEG source accelerating voltage of 200 kV, +/-70 degrees tilted computer-controlled stage and is equipped with a 4K x 4K Eagle CCD Camera with a 4-port readout and 15µm pixel size. EPU software has been used to further study the data.

### Photocatalytic Degradation of Dye

Photocatalytic experiments were carried out using leaf extract of *Smilax aspera* by degrading methylene blue and ethylene orange under solar radiation. To make colloidal suspension of ZnO -NPs with dye, 1 mg dye in 100 ml distilled water was constantly stirred. Then 5 mg ZnO-NPs added in 25 ml of dye solution and kept under instantaneous exposure to Sunlight. Known volume (5ml) was withdrawn at various intervals of time such as 0, 60, 120, 180, 240, 300 minutes and measured using a spectrophotometer at 200-650 nm to assess the rate of degradation. The % degradation was calculated using the equation:

$$\% \text{ Degradation of dye} = (C_i - C_f) \times 100 / C_i$$

Where  $C_i$  &  $C_f$  are the initial and final concentrations of the dye. The same procedure was repeated for different catalytic load of samples (100, 150 and 200 mg) and at different concentration of dye (10, 15 and 20 ppm) keeping the concentration of catalyst constant and also at different pH (viz., 2, 4, 6, 8, 10, 12).

### Antibacterial Assessment

The agar well diffusion method is a rapid and effective test to evaluate the antibacterial activity. Leaf extract were tested against two gram-positive *Staphylococcus aureus*, *Streptococcus pneumoniae* and three gram-negative pathogens *klebsiella pneumoniae*, *Escherichia coli* and *Pseudomonas aeruginosa* respectively [26]. A suspension of Zinc oxide nanoparticles of varying concentrations of 50µg/ml, 100µg/ml and 150µg/ml in 0.5% DMSO was used for screening the antimicrobial activity of nanoparticles against the test microorganisms. DMSO was used as a control and erythromycin has been used as positive control standard antibiotics. Test organisms were dispersed over the surface of agar plates. A small amount of sample is gently pushed over the center of the nutrient agar plate inoculated with bacterial cells from intimate contact of the sample and plates were incubated at 37 °C for 24 h. The antibacterial activity of ZnO nanoparticles was demonstrated by the diameter of the zone of inhibition developed in and around the sample.

### Antioxidant Evaluation

To evaluate the radical scavenging activity of ZnO-NPs antioxidant compound DPPH (2,2- diphenyl-1- picrylhydrazyl) is commonly used in the modified method by Brand-Williams et al. We used various concentrations of ZnO-NPs and standard butylated hydroxytoluene (BHT). In each test sample, 1 mL of freshly prepared DPPH (1 mM) dissolved in methanol solvent was added [27]. Absorbance at 517 nm was measured. The experiments were performed in triplicate and percentage inhibition was calculated from the absorbance of synthesized ZnO-NPs and positive control using the following equation:

$\% \text{ inhibition} = [\text{control OD} - \text{Sample OD}] / \text{Control OD} \times 100$  We further calculated  $IC_{50}$  from the concentration and % inhibition graph.

## Result and Discussion

### UV-visible Spectroscopy

The zinc oxide nanoparticles were synthesized with the Green Nanotechnology approach using leaf extract at 60 °C for 10 min duration for the reduction of zinc acetate to zinc oxide NPs. ZnO-NPs exhibited a peak at 375 nm for phytoextract in the UV-Visible spectra (Figure 5a). The appearance of yellow colour was caused due to the excitation of the surface plasmon vibrations, characteristic of ZnO having 350-400nm visible range which is quite similar to earlier synthesized ZnO-NPs by *Parthenium* leaf extract [28]. The bandgap energy ( $E_g$ ) of ZnO nanoparticles can be evaluated from the UV-Vis spectra by the Tauc plot of  $(h\nu)^2$  v/s  $(h\nu)$  and tangent to X- axis.

Where  $\alpha$  is the absorption coefficient,  $E_g$  is the direct bandgap energy,  $h\nu$  is the photon energy and  $K$  is a constant independent of wavelength.

The absorption coefficient ( $\alpha$ )  $A = I/I_0 = e^{(-\alpha d)}$  can be calculated using the relation deduced from Beer-Lambert's equation, where  $A$  is the absorbance determined from the UV-Visible spectrum and  $d$  is the path length of cuvette. UV-Vis absorption spectra and the Tauc plot of ZnO nanoparticles are shown in Figures 5a and b respectively. The estimated optical band gaps of ZnO-NPs is about 3.19eV [29,30].

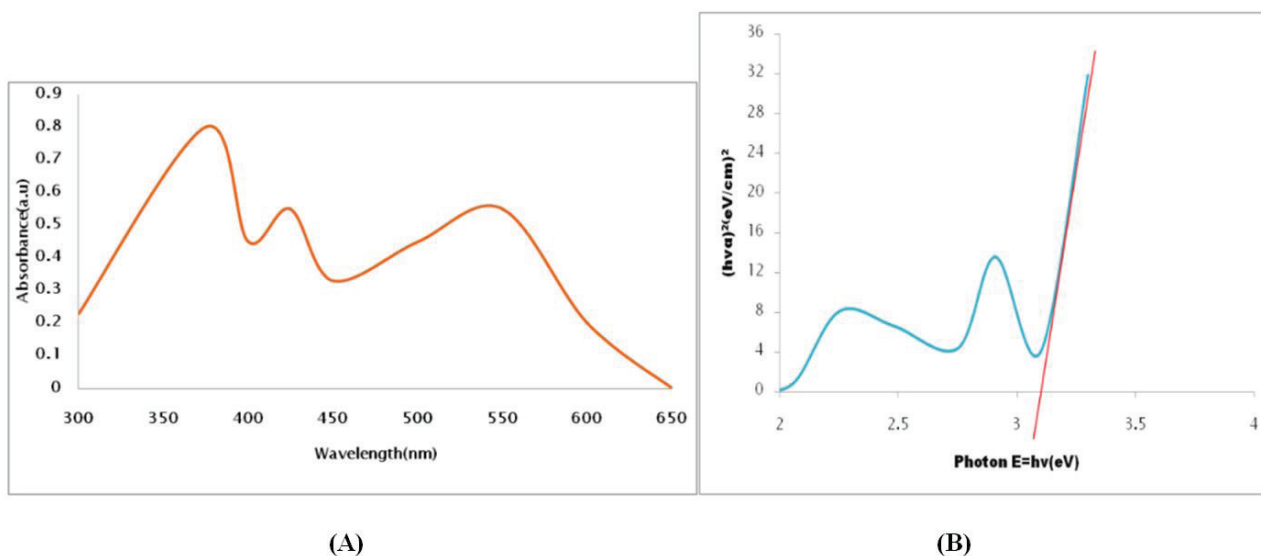


Figure 5: (A): UV absorption spectra; (B): Tauc plot of ZnO-NPs

## XRD Characterization

Powder X-ray diffraction was used to evaluate the structural property and purity of the nanostructured products. XRD revealed the presence of strong, sharp and contracted diffracted patterns pointing towards the crystallite nature of the synthesized zinc oxide nanoparticles. The obtained peaks corresponds to the hexagonal phase in the lattice planes (h,k,l) of (1,0,0), (0,0,2), (1,0,1), (1,0,2), (1,1,0), (1,0,3), (2,0,0), (2,0,1), (1,0,4) having  $2\theta$  value: 31.74,

34.74, 36.22, 47.49, 56.54, 62.78, 66.30, 69.03 and 81.272 (Figure 6). Generally, the broadening of peak in XRD pattern is attributed to the variation in size. The crystallite size is found to be 13.9 nm for leaf extract. Since the spectra does not consist any additional peak it was concluded the sample is in pure form.

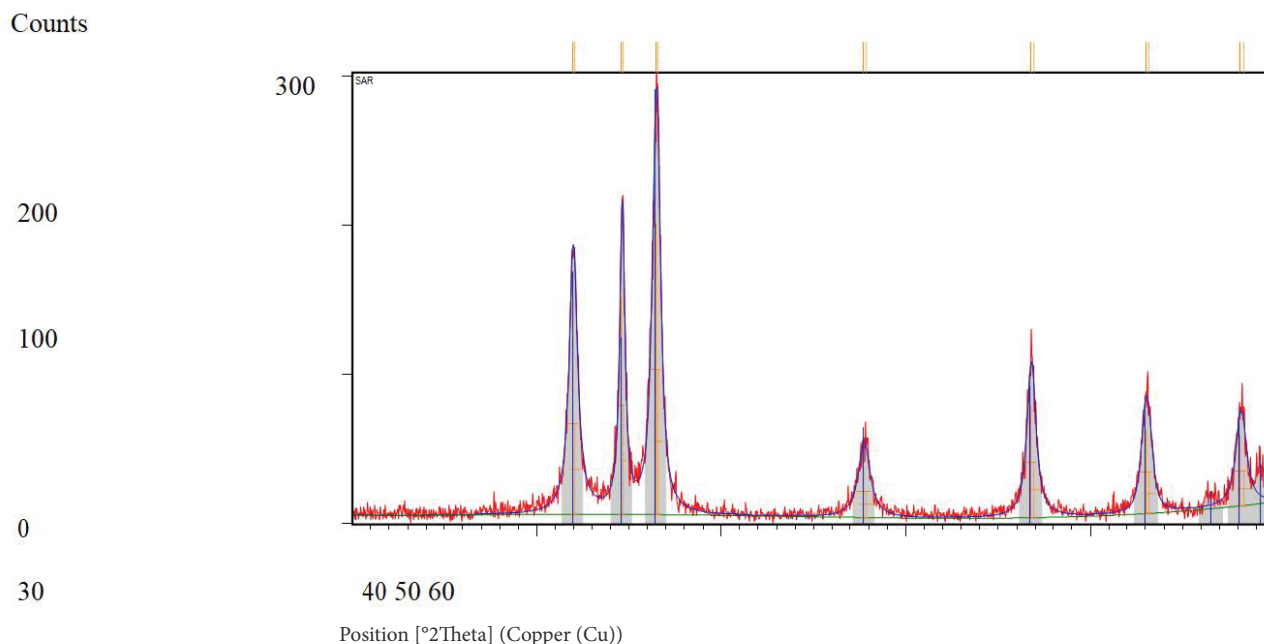


Figure 6: XRD pattern of ZnO-NPs of the leaf extract of *Smilax aspera*

## SEM and EDX Analysis

SEM image is used to identify the morphology of the ZnO Nanoparticles which are displayed in Figures 7a and b under different magnifications. It is observed that most of the nanoparticles are agglomerated and boundary clearly indicated their irregular shapes which might be induced by solvent evaporation during sample grinding and might be responsible for various size distribution.

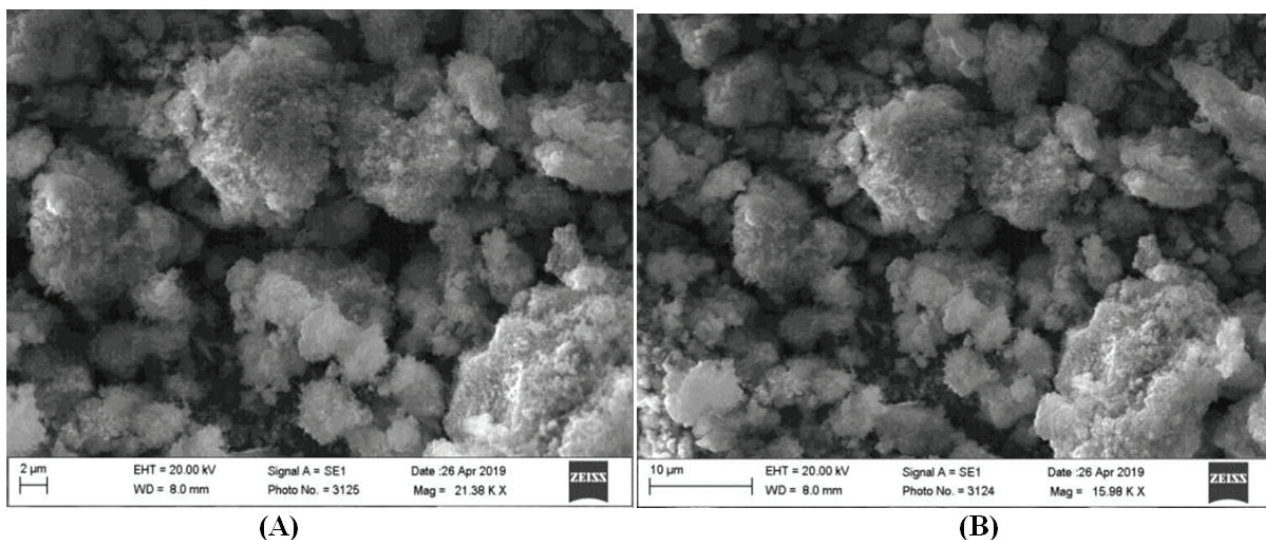


Figure 7: SEM images of ZnO-NPs of Leaf of *Smilax aspera* at different magnification

Further EDX of the powdered samples in Figures 8a and b revealed strong signals confirming the formation of ZnO-NPs. Carbon comes from the artifact during plant extract preparation. The existing peaks are corresponding to Zn and O with a negligible amount of carbon which shows the purity of ZnO nanoparticles.

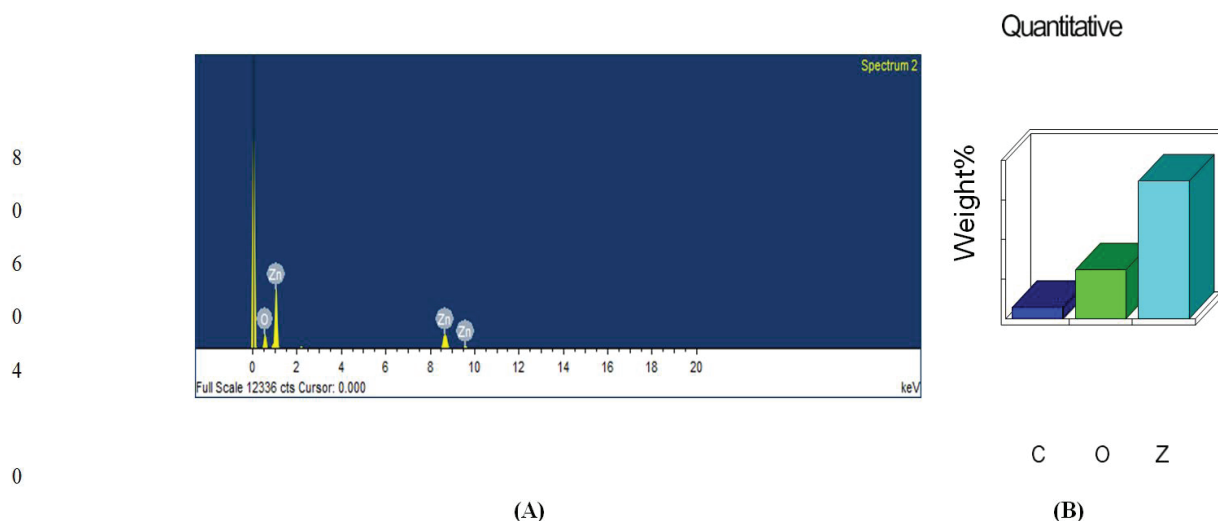


Figure 8: (A): EDX spectrum of the leaf extract of *Smilax aspera*; (B): % Composition

TEM Image Analysis

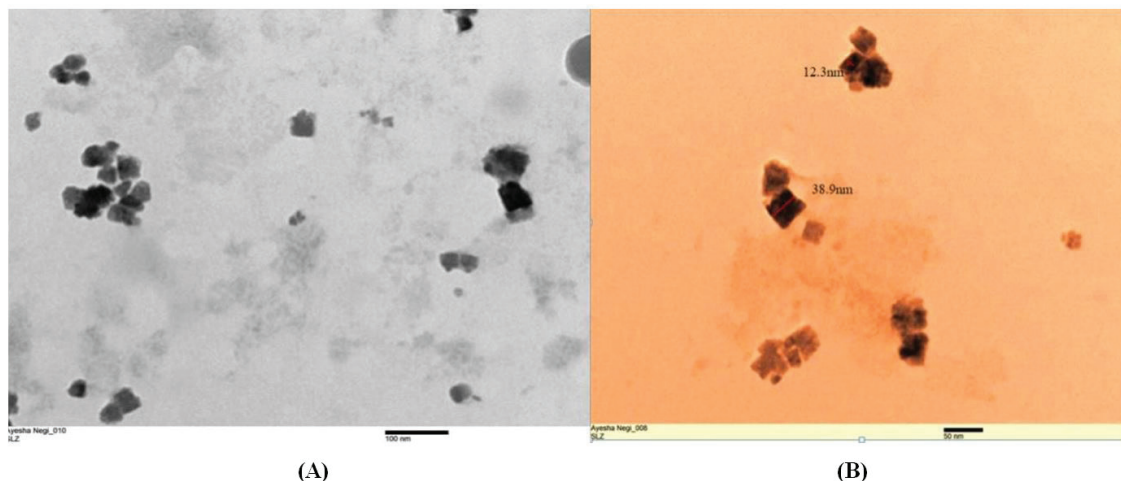


Figure 9: (A and B): TEM image of the leaf extract at different Magnification

Transmission Electron Microscope was used to visualize the size and shape of formed NPs. The characteristic TEM image of ZnO-NPs are shown in Figures 9a and b, which exhibits the agglomerated particles are irregular cubic in shape having a core size 11 nm. The Size was determined dependent on differently magnified images. Further, this sort of morphology has been found in oxide formed in the combustion of the solution.

### Photocatalytic Degradation of Dyes

The photodegradation of MB & MO was determined by normalized change in concentration and degradation efficiency. The normalized concentration change of pure MO was 7.6% following an hour which turned 32% following 5 hours on direct exposure to sunlight. On blending ZnO-NPs the productivity was resolved 31.5% following an hour which on the consistent introduction of solar light following 300 minutes got 49%. For pure MB arrangement degradation efficiency was 25% which after 4 hours went to 41.25%. On blending ZnO-NPs it was observed 27% after 60 minutes, which turned 56.6% after 4 hrs.

The intersection of these two curves ( $C/C_0$  and  $1 - C/C_0$ ) shows the half-life of MB, which is the time taken for initial concentration to remain its half. On mixing ZnO-NPs the half-life was determined at 180 minutes for MO while for MB half-life thus evaluated at 250 minutes.

The above results confirm synthesize ZnO-NPs as an efficient Photodegradative agent (Figures 10 and 11).

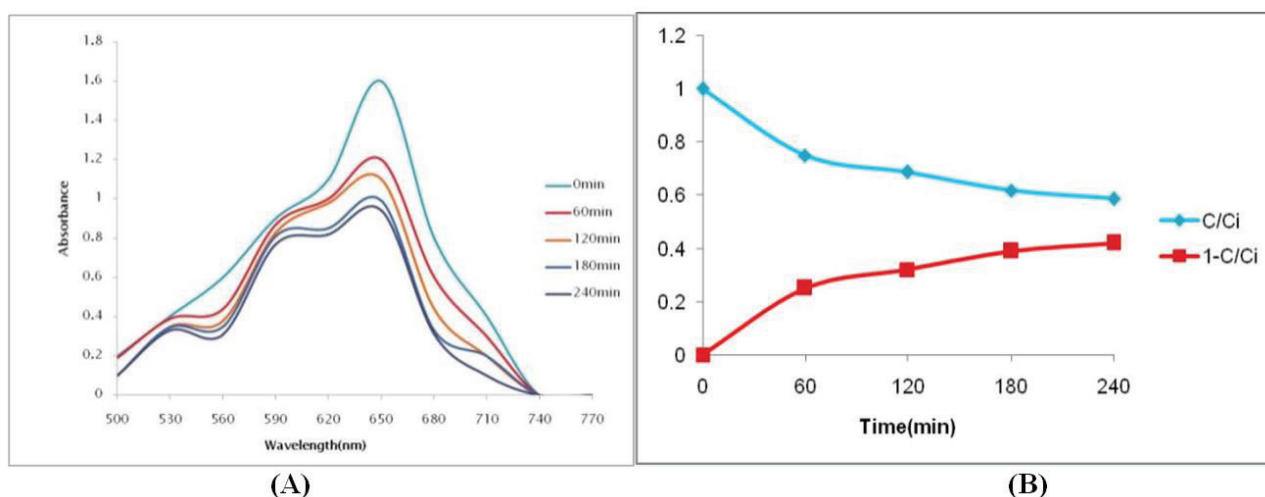


Figure 10: (A): Photodegradation of Pure MB; (B): C/Ci of pure MB

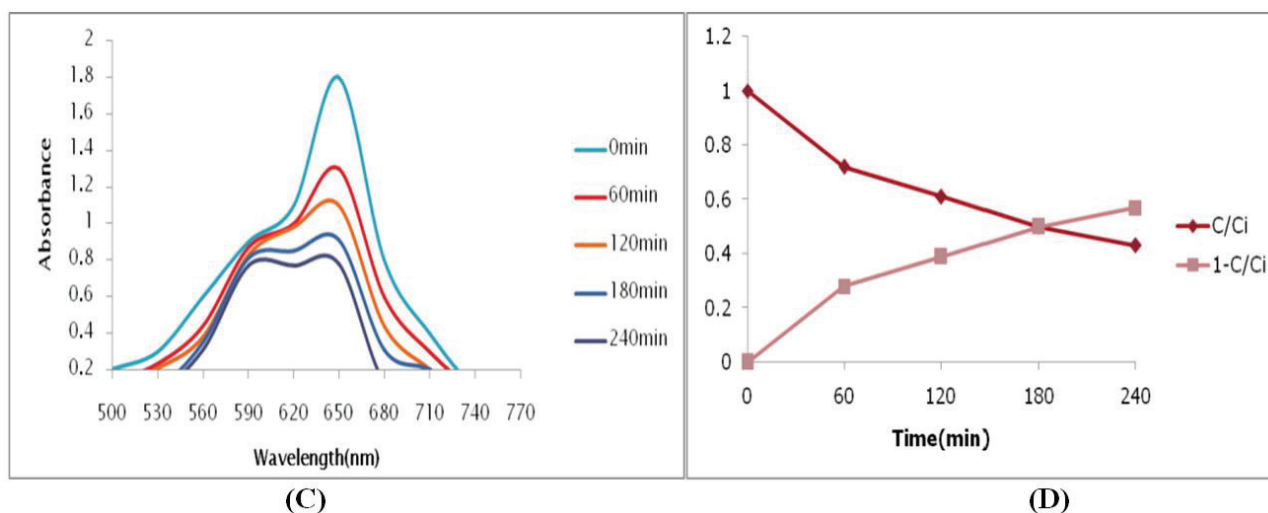
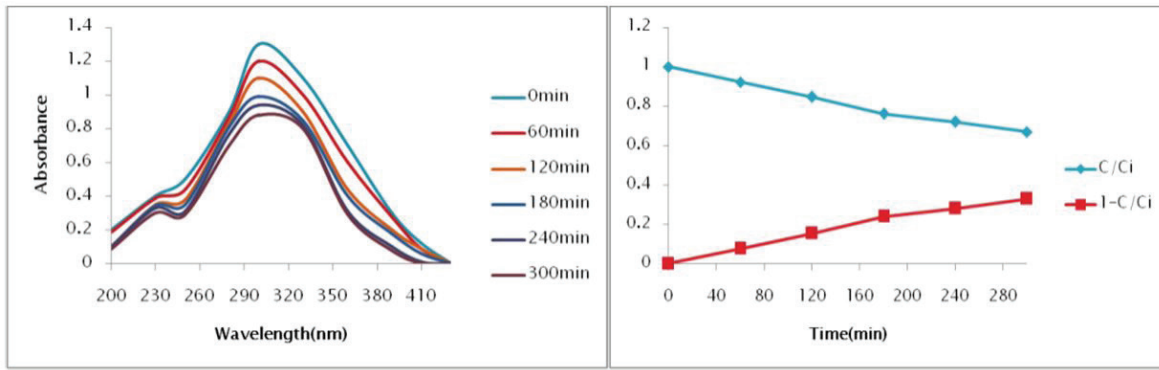
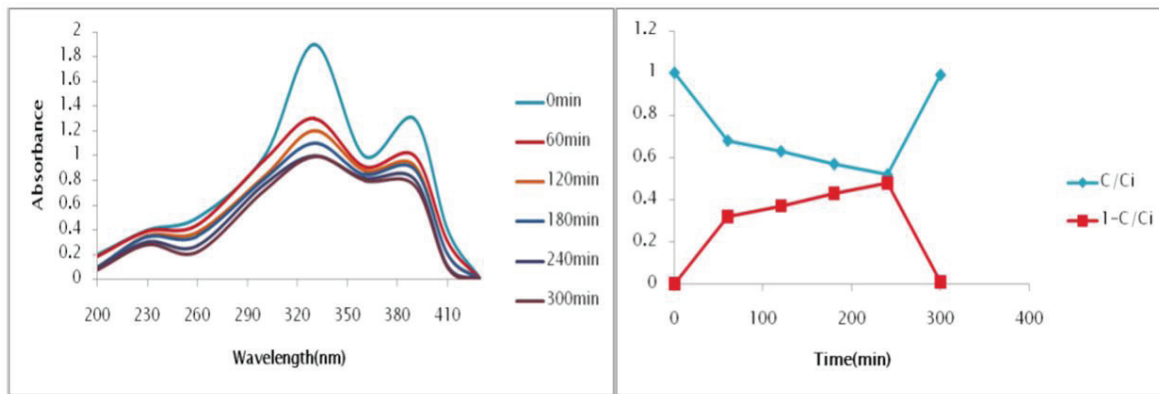


Figure 10: (C): MB degraded by ZnO-NPs; (D): C/Ci of MB using ZnO -NPs

The intersection of these two curves ( $C/C_0$  and  $1 - C/C_0$ ) shows the half-life of MB, which is the time taken for initial concentration to remain its half.



(A) (B)  
Figure 11: (A): Photodegradation of Pure MO; (B): C/Ci of pure MO



(C) (D)  
Figure 11: (C): MO degraded by ZnO-NPs; (D): C/Ci of MO using ZnO-NPs

Antimicrobial Test

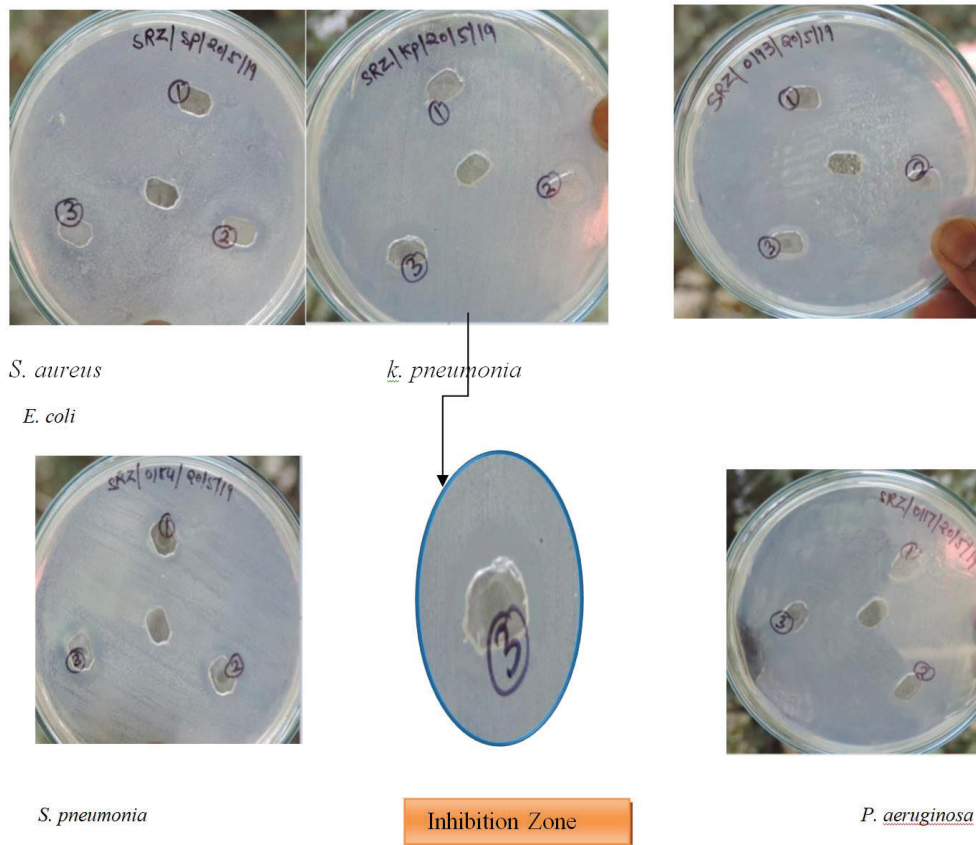


Figure 12: Antibacterial efficacy of ZnO-NPs of the leaf extract of *Smilax aspera*

S.N.	Pathogen	CONTROL	Antibiotic	50 $\mu$ L	100 $\mu$ L	150 $\mu$ L
1.	<i>k. pneumonia</i>	-	15	14mm	16mm	17 mm
2.	<i>S. pneumonia</i>	-	18	14mm	15mm	16mm
3.	<i>E. coli</i>	-	-	16mm	18 mm	20 mm
4.	<i>P. aeruginosa</i>	-	10	-	-	-
5.	<i>S. aureus</i>	-	14.5	14mm	16 mm	17 mm

**Table 1:** Antibacterial evaluation of ZnO-NPs of the leaf extract of *Smilax aspera* Cork diameter- 8mm

Highlighted results showed synthesized ZnO-NPs has better antibacterial activity than market available drug and can be used as an alternative (Figure 12) and (Table 1).

### DPPH radical scavenging assessment

DPPH is a steadier and more eminent free radical based on accepting hydrogen or electron from donors. The color of the DPPH solution steadily changes from purple to light yellow in presence of ZnO nanoparticles hence the peak intensity from 517 nm gradually decreases. The study was carried out at different concentrations of ZnO-NPs solution such as 1, 2, 3 mg/ml. BHT solution used as positive control at 1-3 mg/ml concentrations. The obtained results are shown in Figures 13a and b. We recorded that the activity increased with concentration of ZnO-NPs solution. Using 1, 2, 3 mg/ml correspondingly 81.9%, 84.7%, 94.3% values were  $IC_{50}$ =3.9mg/ml attributed to BHT, synthesized ZnO-NPs with  $IC_{50}$ = 7.26mg/ml for leaf part has been evaluated. Synthesized ZnO-NPs using leaf has better antioxidant activity.

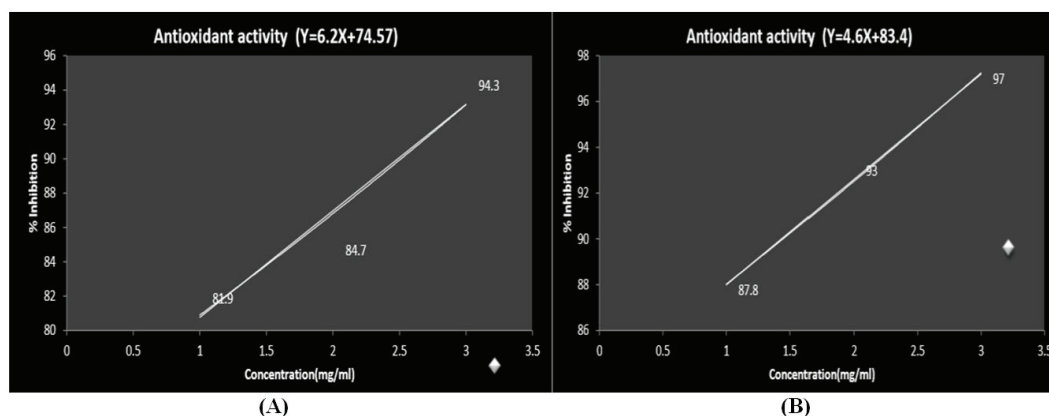


**Figure 13:** (A): Antioxidant activity of BHT; (B): Antioxidant activity of ZnO-NPs

### Conclusion

The novel fabrication of ZnO nanoparticles was achieved using a plant with verified advantages as they are easily available, nontoxic, and consists phytoconstituents which plays role of reducing or capping agent for the formation of NPs. Hexagonal phase ZnO-NPs using leaf of *Smilax aspera* at 60 °C formed with in core size limited about 12 nm is characterized by XRD, SEM and TEM. The evaluation of photocatalytic activity may be considered the photocatalyst NP as a heterogeneous photocatalysis to tackle water contamination and reduce environmental pollution. This biosynthesized ZnO-NPs have been introduced as a potential free radical scavenger while comparing to standard antioxidants and portrayed exceptionally well antibacterial activity. Deeming everything, our outcome exhibits the enhancement of a speedy, inexpensive, biodegradable and protected approach of ZnO-NPs for fighting against bacterial infections and environmental pollution.

### Acknowledgement

The research work was financially supported by University Grants Commission, New Delhi. Thanks, are also due to All India Institute of Medical Sciences, New Delhi (India) for TEM studies and USIC, HNB Garhwal University for XRD, EDS, and SEM facilities, respectively.

### References

- Jiang R, Zhu H, Li X, Xiao L (2009) Visible light photocatalytic decolorization of CI Acid Red 66 by chitosan capped CdS composite Nanoparticles. Chem Eng Trans 152: 537-42.
- Sharma M, Jain T, Singh S, Pandey OP (2012) Photocatalytic degradation of organic dyes under UV- Visible light using capped ZnS Nanoparticles. Solar Energy 86: 626-33.
- Torres-Martínez CL, Kho R, Mian OI, Mehra RK (2001) Efficient photocatalytic degradation of environmental pollutants with mass-produced ZnS nanocrystals. J Colloid Interface Sci 240: 525-32.
- Zhu H, Jiang R, Xiao L, Chang Y, Guan Y, et al. (2009) Photocatalytic decolorization and degradation of Congo Red on innovative crosslinked chitosan/nano-CdS composite catalyst under visible light irradiation. J Hazard Mater 169: 933-40.

5. Wang R, Xu D, Liu J, Li K, Wang H (2011) Preparation and photocatalytic properties of CdS/La<sub>2</sub>Ti<sub>2</sub>O<sub>7</sub> nanocomposites under visible light. *Chem Eng Sci* 168: 455-60.
6. Suresh D, Shobharani RM, Nethravathi PC, Kumar MP, Nagabhushana H, et al. (2015) Artocarpus gomezianus aided green synthesis of ZnO nanoparticles: luminescence photocatalytic and antioxidant properties *Spectrochimica Acta Part A: Molecular and Biomolecular Spectroscopy* 141: 128-34.
7. Ijaz F, Shahid S, Khan SA, Ahmad W, Zaman S (2017) Green synthesis of copper oxide nanoparticles using *Abutilon indicum* leaf extract: Antimicrobial, antioxidant and photocatalytic dye degradation activities *Tropical Journal of Pharmaceutical Research* 16: 743-53.
8. Sirelkhatim A, Mahmud S, Seeni A, Kaus NHM, Ann LC, et al. (2015) Review on zinc oxide nanoparticles: antibacterial activity and toxicity mechanism. *Nano-micro letters* 7: 219- 42.
9. Nethravathi PC, Kumar MP, Suresh D, Lingaraju K, Rajanaika H, et al. (2015) *Tinospora cordifolia* mediated facile green synthesis of cupric oxide nanoparticles and their photocatalytic antioxidant and antibacterial properties. *Mater Sci Semicond Process* 33: 81- 8.
10. Robertson N (2006) Optimizing dyes for dye-sensitized solar cells. *Angewandte Chemie International Edition* 45: 2338-45.
11. He W, Kim HK, Wamer WG, Melka D, Callahan JH, et al. (2014) Photogenerated charge carriers and reactive oxygen species in ZnO/Au hybrid nanostructures with enhanced photocatalytic and antibacterial activity. *J Am Chem Soc* 136: 750-7.
12. Parmar A, Kaur G, Kapil S, Sharma V, Sachar S (2019) Green chemistry mediated synthesis of PLGA- Silver nanocomposites for antibacterial synergy: Introspection of formulation parameters on structural and bactericidal aspects. *Reactive and Functional Polymers* 141: 68-81.
13. Tolera M, Abate D, Dheresa M, Marami D (2018) Bacterial nosocomial infections and antimicrobial susceptibility pattern among patients admitted at hiwot fana specialized university hospital Eastern Ethiopia. *Advances in medicine* 2018: 10.1155/2018/2127814.
14. Okeke IN, Laxminarayan R, Bhutta ZA, Duse AG, Jenkins P, et al. (2005) Antimicrobial resistance in developing countries. Part I: recent trends and current status. *Lancet Infect Dis* 5: 481-93.
15. Shehab N, Patel PR, Srinivasan A, Budnitz DS (2008) Emergency department visits for antibiotic- associated adverse events. *Clin Infect Dis* 47: 735-43.
16. Zhang J, Wang H, Wang L, Ali S, Wang C, et al. (2019) Wet-chemistry strong metal- support interactions in titania-supported Au Catalysts. *J Am Chem Soc* 141: 2975-83.
17. Khoobchandani M, Saxena A (2019) Targeted phytochemical-conjugated gold nanoparticles in cancer treatment In: *Biotechnology Products in Everyday Life*, Springer, USA.
18. El-Rafie HM, Zahran MK (2013) Green synthesis of silver nanoparticles using polysaccharides extracted from marine macro algae. *Carbohydrate Polymers* 96: 403-10.
19. Aayasha N, Prachi, Mahender S, Negi DS (2019) A review on eco-friendly synthesis and application of metal nano particles using medicinal plants. *Int J Basic Appl Res* 9: 491-510.
20. Prathna TC, Chandrasekaran N, Raichur AM, Mukherjee A (2011) Kinetic evolution studies of silver nanoparticles in a bio-based green synthesis process. *Colloids and Surfaces A: Physicochemical and Engineering Aspects* 377: 212-6.
21. Zheng Y, Fu L, Han F, Wang A, Cai W, et al. (2015) Green biosynthesis and characterization of zinc oxide nanoparticles using *Corymbia citriodora* leaf extract and their photocatalytic activity. *Green Chemistry Letters and Reviews* 8: 59-63.
22. Longo L, Vasapollo G (2006) Extraction and identification of anthocyanins from *Smilax aspera* L. berries. *Food Chemistry* 94: 226-31.
23. Belhouchet Z, Sautour M, Miyamoto T, Lacaille-Dubois MA (2008) Steroidal Saponins from the Roots of *Smilax aspera* subsp. *Mauritanica*. *Chem Pharm Bull (Tokyo)* 56: 1324-7.
24. Delgado-Pelayo R, Hornero-Méndez D (2012) Identification and quantitative analysis of carotenoids and their esters from sarsaparilla (*Smilax aspera* L.) berries. *J Agric Food Chem* 60: 8225-32.
25. Selmi H, Hammami O, Dhifallah A, Jedidi S, Dallali S, et al. (2012) Phytochemical Screening Antioxidant Activity And In Vitro Fermentation From *Smilax aspera* *Rhamnus Alaternus* And *Calycotum Villosa* From Ewes And Goats. 'Proceeding Book' 304.
26. Andrews JM (2001) Determination of minimum inhibitory concentrations. *J Antimicrob Chemother* 48: 5-16.
27. Brand-Williams W, Cuvelier ME, Berset C (1995) Use of a free radical method to evaluate antioxidant activity. *LWT-Food science and Technology* 28: 25-30.
28. Rajiv P, Rajeshwari S, Venkatesh R (2013) Bio-Fabrication of zinc oxide nanoparticles using leaf extract of *Parthenium hysterophorus* L. and its size-dependent antifungal activity against plant fungal pathogens. *Spectrochimica Acta Part A: Molecular and Biomolecular Spectroscopy* 112: 384-7.
29. Simmons BA, Li S, John VT, McPherson GL, Bose A, et al. (2002). Morphology of CdS nanocrystals synthesized in a mixed surfactant system. *Nano Letters* 2: 263-8.
30. Seoudi R, Shabaka A, Eisa WH, Anies B, Farage NM (2010) Effect of the prepared temperature on the size of CdS and ZnS nanoparticle. *Physica B: Condensed Matter* 405: 919-24.

Submit your next manuscript to Annex Publishers and benefit from:

- ▶ Easy online submission process
- ▶ Rapid peer review process
- ▶ Online article availability soon after acceptance for Publication
- ▶ Open access: articles available free online
- ▶ More accessibility of the articles to the readers/researchers within the field
- ▶ Better discount on subsequent article submission

Submit your manuscript at

<http://www.annexpublishers.com/paper-submission.php>